FREQUENCY COMPARISON (H_MASER 40 0890) - (LNE-SYRTE-FO2)
From MJD 53764 to MJD 53789

The primary frequency standard LNE-SYRTE-FO2 was compared to the hydrogen Maser (40 0890) of the laboratory, from MJD 53789 to MJD 53789.

Period (MJD)	**y(HMaser$_{40\ 0890}$ - FO2)** (6)	u_B (2)	u_A (6)	$u_{link\ /\ maser}$ (4)
53764 – 53789	**- 1853,03**	**6,11**	**1,53**	**1,03**

Table 1: Results of the comparison in 1 x 10^{-16} unit.

Figure 1 collects the measurements of fractional frequency differences during the 29th January to 23rd February 2006 period. Error bars represent the combined statistical and systematic uncertainties. The measurements are corrected for the systematic frequency shifts listed below.

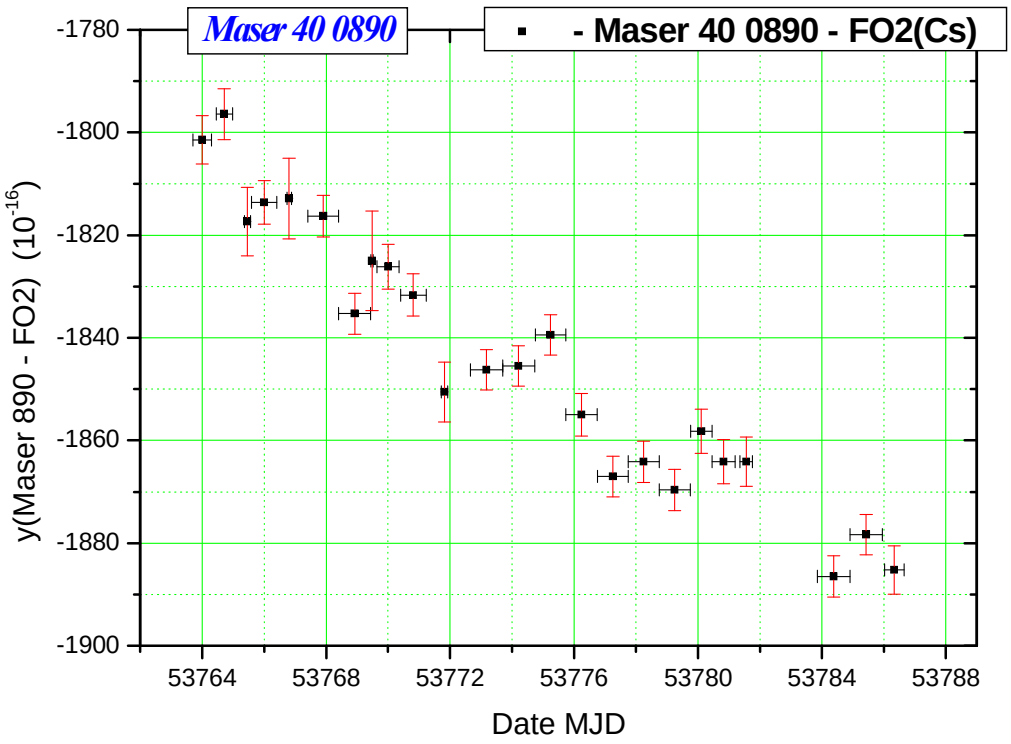

Figure 1: fractional frequency differences between H_Maser40 0890 & FO2 from MJD 53764 to MJD 53789

Table of measurements is given bellow (table 2) and a synthesis of calculation on table 3.

Start UTC dates unit MJD	Stop UTC dates unit MJD	Duration H :M	Mean fractional frequency differences $y_{Maser} - y_{FO2}$	type A uncertainties	
				σ_{Stat}	$\sigma_{Collision}$
53763,70417	53764,30903	14:31	-1,80144E-13	2,24E-16	2,75E-16
53764,45694	53764,97431	12:25	-1,79641E-13	2,5E-16	2,93E-16
53765,36667	53765,55556	04:32	-1,81734E-13	3,6E-16	4,68E-16
53765,59375	53766,40764	19:32	-1,81363E-13	1,85E-16	2,16E-16
53766,73194	53766,88611	03:42	-1,81288E-13	4,68E-16	5,45E-16
53767,40833	53768,40556	23:56	-1,81633E-13	1,64E-16	2,02E-16
53768,40556	53769,44236	24:53	-1,83530E-13	1,6E-16	1,95E-16
53769,44722	53769,52153	01:47	-1,82499E-13	5,67E-16	7,26E-16
53769,64167	53770,36111	17:16	-1,82614E-13	1,96E-16	2,37E-16
53770,40000	53771,22778	19:52	-1,83167E-13	1,74E-16	2,08E-16
53771,72292	53771,92292	04:48	-1,85056E-13	3,16E-16	3,78E-16
53772,66181	53773,69375	24:46	-1,84623E-13	1,57E-16	1,87E-16
53773,69375	53774,72778	24:49	-1,84549E-13	1,55E-16	1,87E-16
53774,75486	53775,73403	23:30	-1,83944E-13	1,56E-16	1,89E-16
53775,73403	53776,75000	24:23	-1,85499E-13	1,75E-16	2,15E-16
53776,75833	53777,75069	23:49	-1,86703E-13	1,61E-16	1,95E-16
53777,75069	53778,74583	23:53	-1,86415E-13	1,69E-16	2,04E-16
53778,74583	53779,75139	24:08	-1,86964E-13	1,66E-16	1,99E-16
53779,75903	53780,45556	16:43	-1,85823E-13	1,87E-16	2,31E-16
53780,45556	53781,20556	18:00	-1,86415E-13	1,89E-16	2,31E-16
53781,35625	53781,76042	09:42	-1,86413E-13	2,28E-16	2,85E-16
53783,85556	53784,90139	25:06	-1,88649E-13	1,62E-16	1,96E-16
53784,90139	53785,94653	25:05	-1,87831E-13	1,54E-16	1,9E-16
53786,01597	53786,65208	15:16	-1,88525E-13	2,24E-16	2,77E-16
53789,00000					

Table 2: Measurements H_Maser40 0890 - FO2 from MJD 53764 to MJD 53789

Dates Duration & Measurement Rate	Mean frequency difference normalized $y_{Maser} - y_{FO2}$ **(1)**	type A uncertainty σ_{Stat} & $\sigma_{Collision}$	Uncertainty due to the dead times $\sigma_{deadTime}$ **(4)**
Start date MJD UTC 53763,70417 Stop date MJD UTC 53786,65208 Total duration : 22,9479 d Total measurements 17,766 d Measurement Rate: 77,42% τ_0 = 82612 s	Standard Mean $\bar{y}$ = **- 1843,76 x 10^{-16}** Weighted Mean **(5)**: $\bar{y}$ = **- 1848,38 x 10^{-16}** Linear fit regression **(6)**: $\bar{y}$ = **- 1853,03 x 10^{-16}** High order polynomial fit **(6)**: $\bar{y}$ = **- 1843,33 x 10^{-16}** Mean from Phase differences **(7)**: $\bar{y}$ = **- 1848,23 x 10^{-16}**	Standard deviation **S_d = 26,24 x 10^{-16}** By Weighted Mean **(5)** σ_A = **0,61 x 10^{-16}** By Linear fit regression**(6)** σ_y = **1,53 x 10^{-16}** By High order Polynomial fit **(6)** σ_y = **0,64 x 10^{-16}** From Phase differences **(7)** σ_A = **0,47 x 10^{-16}**	$\sigma_{deadTime}$ = **0,27 10^{-16}**

Table 3: Statistics of measurements

The frequency mean calculated by other method than (6) show a difference of about $1x10^{-15}$ due to the time interval of measurements that was finished at MJD 53786,65 while the BIPM time interval is finished at MJD 53789.

(1) Fractional frequency difference obtained after systematic relative frequency shifts correction:

$$y_{Maser-FO2} = \frac{(\delta(\nu))_{Zeeman2}}{\nu_0} + \frac{(\delta(\nu))_{BlackBody}}{\nu_0} + \frac{(\delta(\nu))_{Collision+CavityPulling}}{\nu_0} + \frac{(\delta(\nu))_{redshift}}{\nu_0} - \frac{f_{mesure}}{\nu_0}$$

with $\nu_0 := 0.9192631770 \ \ 10^{10}$. The fractional mean frequency is calculated by four ways as mentioned in table 3 in order to have comparison between statistical computation such as standard mean, weighted mean, with a linear fit and with phase differences.

(2) Systematic uncertainty $\sigma_B = u_B$ in which statistical effect of cold collisions and cavity pulling is removed (see **Annex 1**)

$$\sigma_B = \left(\sigma_{Zeeman2}^2 + \sigma_{BlackBody}^2 + \sigma_{Collision_{Syst}}^2 + \sigma_{Microwave\_Spectrum}^2 + \sigma_{Microwave\_Leakage}^2 + \sigma_{Ramsey\_Rabi}^2 + \sigma_{Recoil}^2 + \sigma_{second\_Doppler}^2 + \sigma_{Background\_collsions}^2 + \sigma_{Redshift}^2 \right)^{(1/2)}$$

(3) Statistical uncertainty $\sigma_A = u_A$, in which is taken into account the statistical uncertainty on each measurement σ_{Stat_i} and statistical effect on the cold collisions and Cavity Pulling measurement $\sigma_{Collision_i}$ (see **Annex 4** Linear Regression on the frequency measurements & **Annex 5**) : $\sigma_A = \sqrt{\frac{1}{\sum_{i=1}^{n} \frac{1}{\sigma_{Stat_i}^2 + \sigma_{Collision_i}^2}}}$

(4) Uncertainty due to the link between H_Maser and the fountain FO2 $u_{link\_Maser} = \sqrt{\sigma_{link\_Lab}^2 + \sigma_{dead\_time}^2}$ where $\sigma_{link\ lab} := 1.\ 10^{-16}$ and σ_{dead_time} is the uncertainty due to the dead times during measurements (see **Annex 3**)

(5) Weighted Mean by statistical uncertainty on each measurement

$$y_j := \frac{\sum_{i=1}^{n_j} \frac{y_i}{\sigma_{Ai}^2}}{\sum_{i=1}^{n_j} \frac{1}{\sigma_{Ai}^2}}$$

where $\sigma_A = \sqrt{\frac{1}{\sum_{i=1}^{n} \frac{1}{\sigma_{A_i}^2}}}$ with $\sigma_{A_i} = \sqrt{\sigma_{Stat_i}^2 + \sigma_{Collision_i}^2}$

(6) Mean frequency obtained by a linear fit by weighted least squares with statistical uncertainty on each measurement and by an high order polynomial fit (see **Annex 4**).

(7) Mean frequency obtained by phase differences (see **Annex 5**).

ANNEX 1

Uncertainties of systematic effects in the FO2 fountain

Systematic effects taken into account are the quadratic Zeeman, the Black Body, the cold collision and cavity pulling corresponding to the systematic part (see Annex 2), the microwave spectral purity and the microwave leakage, the Ramsey Rabi pulling, the recoil, the 2nd Doppler and the background collisions. Each of these effects is affected by an uncertainty. The uncertainty of the red shift effect is also included in the systematic uncertainty budget and gives

$$\sigma_B = \left(\sigma_{Zeeman2}^{\ 2} + \sigma_{BlackBody}^{\ 2} + \sigma_{Collision_{Syst}}^{\ 2} + \sigma_{Microwave\_Spectrum\_Leakage}^{\ 2} + \sigma_{first\_Doppler}^{\ 2} + \sigma_{Ramsey\_Rabi}^{\ 2} + \sigma_{Recoil}^{\ 2} + \sigma_{second\_Doppler}^{\ 2} + \sigma_{Background\_collisions}^{\ 2} + \sigma_{Redshift}^{\ 2} \right)^{(1/2)}$$

Here are mentioned the uncertainties of the different effects (see **Annex 2** and **[ref, 1]**):

Quadratic Zeeman effect	:	$\sigma_{Zeeman2} = 8.038\ 10^{-18}$	(continuously measured)
Black Body effect	:	$\sigma_{Blackbody} = 6.\ 10^{-17}$	(calculated)
Systematic Collisional effect	:	$(\sigma_{Collision})_{Syst} = 2.12\ 10^{-16}$	(continuously measured see annex 2)
Microwave Spectrum purity & Leakage effect	:	$\sigma_{MicrowaveSpectrumLeakage} := 4.3\ 10^{-16}$	(measured)
First order Doppler effect	:	$\sigma_{firstDoppler} := 3.0\ 10^{-16}$	(calculated and measured)
Rabi-Ramsey effect	:	$\sigma_{RabiRamsey} := 1.0\ 10^{-16}$	(calculated)
Recoil effect (see **[ref, 3]**)	:	$\sigma_{recoil} := 1.4\ 10^{-16}$	(calculated)
Second order Doppler effect	:	$\sigma_{SecondDoppler} := 8.\ 10^{-18}$	(calculated)
Background effect	:	$\sigma_{BackGroundCollisions} := 1.\ 10^{-16}$	(evaluated)
Red shift effect	:	$\sigma_{RedShift} := 1.\ 10^{-16}$	(calculated)

For the whole April-May 2005 period it gives

➔ $\sigma_B = 6.11\ 10^{-16}$

ANNEX 2

1 - Measurement of the collisional frequency shift and the cavity pulling

Collisional shift takes into account the effect of the collisions between cold Caesium atoms and the effect of "Cavity Pulling" whose influence also depends on the number of atoms. This effect is measured in a differential way during each integration and its determination thus depends on the duration of the measurement and on the stability of the clock, thus the uncertainty on the determination of the collisional shift is mainly of statistical nature. To the statistical uncertainty, we add a type B uncertainty of 1% of frequency shift resulting from the imperfection of the adiabatic passage method (see the article **[ref. 4]**).

Figure 2 visualizes the relative frequency shift due to the effect of the collisions and "Cavity Pulling" of the atomic fountain FO2 taken in low density, between the MJD 53764 and 53789 with the statistical uncertainty of each measurement, $\sigma_{Collision(i)}$ given in table 2.

Figure 3 shows the Allan deviation of a differential measurement using high and half atom density fountain configurations during MJD 53764 to MJD 53789, in order to correct of the cold collisional shift for this period. FO2 was operated alternatively (every 50 clock cycles) at low atomic density (red diamond) and high density (black square) against the cryogenic oscillator weakly phase locked on the H_Maser890. The measured density ratio between low and high densities is **0,50024478 ± 0,0000352**. The frequency difference between both densities is used to determine the collisional coefficient which is used to correct each data point. The green triangle points represent the Allan deviation of the frequency difference between low and high densities when the points are corrected. The Allan deviation varies as $\tau^{-1/2}$ and reaches 10^{-16} after 100000s.

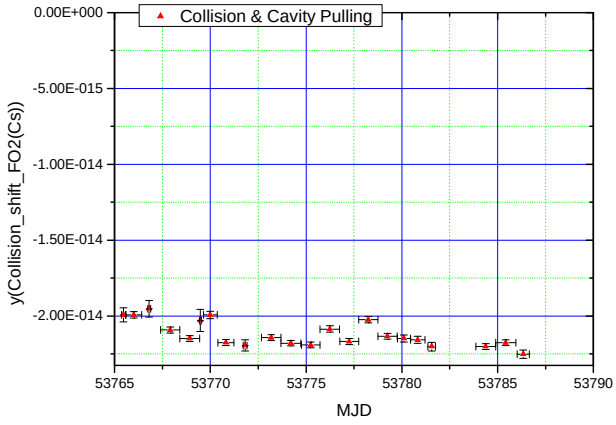

Figure 2: Fractional frequency shift due to cold collisions and Cavity Pulling from MJD 53764 to MJD 53789

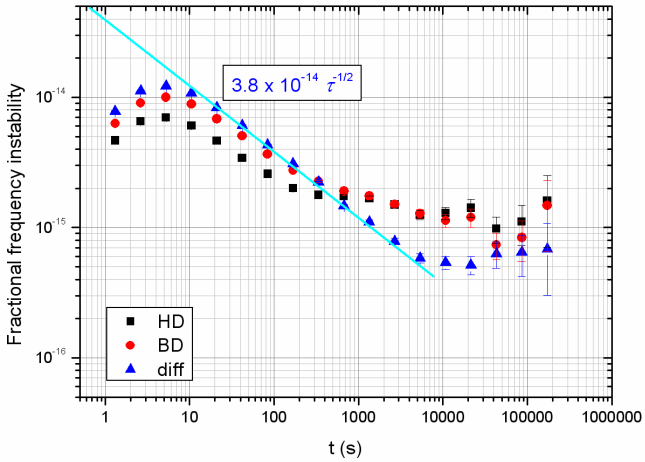

Figure 3: Allan deviation of measurements of the shift frequency in high and low atom density and their differences during MJD 53764 to MJD 53789

The weighted mean $y_{Collision\ moy} = \dfrac{\sum_{i=1}^{n} \dfrac{y_{Collision\ i}}{\sigma_{Collision\ i}^{2}}}{\sum_{i=1}^{n} \dfrac{1}{\sigma_{Collision\ i}^{2}}}$ of collisionnal shift gives for January February 2006

is $y_{Collision_{moy}} := -2.12240\ 10^{-14}$

The systematic effect of these shifts is evaluated by the 1% part of the mean frequency collisional shift during January February 2006:

$$\sigma_{Collision\ Syst} = \frac{1}{100} \left| y_{Collision\ moy} \right| = \boxed{(\sigma_{Collision})_{Syst} = 2.1224\ 10^{-16}}$$

This value is taking into account in the systematic uncertainty evaluation σ_B (see Annex 1).

2 - Measurement of the 2nd order Zeeman frequency shift

Every 20 minutes the frequency of the central fringe of the field linearly dependant transition $|F=3, m_F=1\rangle \longrightarrow |F=4, m_F=1\rangle$ is measured. This frequency is directly proportional to the field as $\delta(\nu_{11})=K_{Z1}B$ with K_{Z1} = 7,0084 Hz.nT^{-1} (see **[ref. 5]** vol. 1 p37 table 1.1.7(a)). In the fountain, the transition $|F=3, m_F=0\rangle \longrightarrow |F=4, m_F=0\rangle$ is shifted by quadratic Zeeman effect and depend on squared magnetic field as $\delta(\nu_{00})=K_{Z2}B^2$ with K_{Z2} = 42,745 mHz.µT^{-2} (see **[ref. 5]** vol. 1 p37 table 1.1.7(a)). Knowing K_{Z1} and measuring δ(ν11) allow good estimation of Zeeman quadratic shift as $\delta(\nu_{00}) = K_{Z2}\left(\frac{\delta(\nu_{11})}{K_{Z1}}\right)^2$. The relative quadratic Zeeman frequency shift is calculated by $\frac{\delta(\nu_{00})}{\nu_0} = \frac{427{,}45\times10^{-6}\left(\frac{\delta(\nu_{11})}{700{,}84}\right)}{\nu_0}$ with $\delta(\nu_{11})$ in Hz unit and ν_0 = 9192631770 Hz. And the uncertainty is evaluated by $\frac{\Delta(\delta(\nu_{00}))}{\nu_0} = 427{,}45\times10^{-6}\times\frac{2\times\overline{B}\times\Delta(B)}{\nu_0}$ with B in mG and $\Delta(B)$ the standard deviation of the magnetic field. Figure 4 displays the tracking of the central fringe during MJD 53764 to MJD 53789. This shows the good stability of the magnetic field in the interrogation zone (the step of the central fringe of -0,6Hz don't affect the stability in an average time interval of one day). The frequency variation is taken as in the first time interval 53764 to 53782, standard deviation **±0.031109Hz** and the second time interval 53783 to 53789, standard deviation **±0.02184199Hz**. For the whole period the standard deviation is **±0,0298549Hz** When taking the standard deviation of variation of the magnetic field $\Delta(B)$ over the whole period of measurement as the field uncertainty, we find **4,26pT**. The corresponding uncertainty of the correction of the second order Zeeman effect is **8,038x10^{-18}**. During each period of about 24h of integration (see table 2) an evaluation of the Zeeman effect is calculated assorted with an uncertainty averaged from the tracking of the central fringe during this interval duration of about 24h.

For $M1 := 1421.94198$ Hz, relative quadratic Zeeman shift $\frac{(\delta(f))_{Zeeman2}}{\nu_0} = 1.914130078\ 10^{-13}$

$$\sigma\left(\frac{(\delta(f))_{Zeeman2}}{\nu_0}\right) = 8.038\ 10^{-18} \rightarrow \boxed{\sigma_{Zeeman2} = 8.038\ 10^{-18}}$$

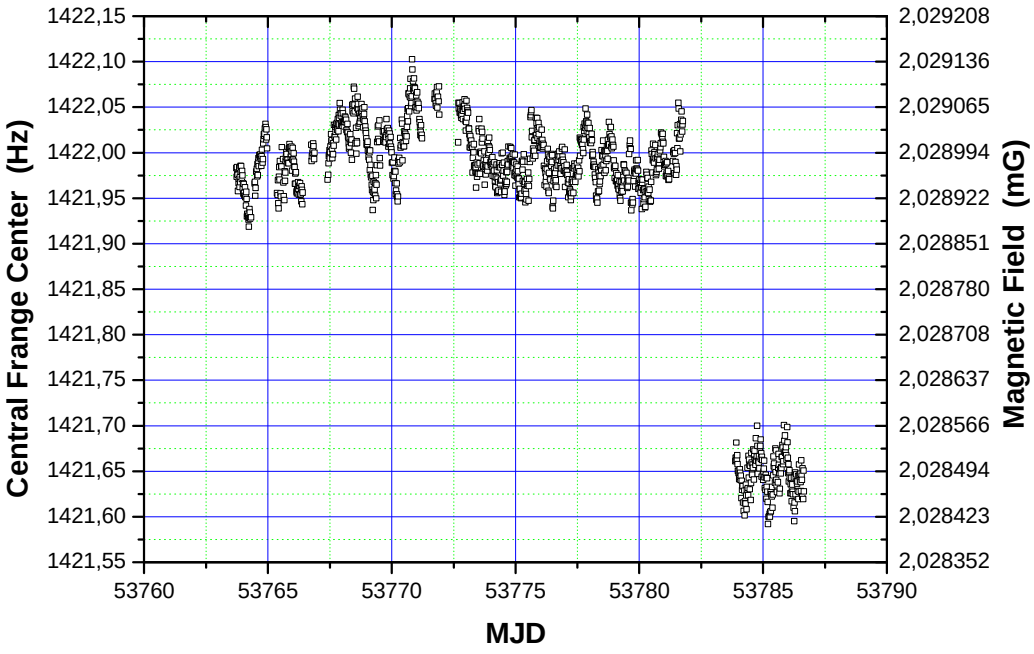

Figure 4: tracking of the central fringe from MJD 53764 to MJD 53789

3 - Measurement of the Blackbody Radiation shift

An ensemble of 3 platinum thermistors monitors the temperature and its gradient inside the vacuum chamber. The average temperature is T~24,5°C with a gradient smaller than $\delta(T) = 0.2\,K$ along the atom trajectory. The correction is

$$\left(\frac{\delta(\nu)}{\nu_0}\right)_{Blackbody} = \frac{K_{BB}\,T^4\left(1+\frac{\varepsilon\,T^2}{T_0^2}\right)}{T_0^4}$$

with $K_{BB} := -1.711\ 10^{-14}\&+\text{-}3.2\ 10^{-17}$ **[ref. 10]**, $\varepsilon := 0.014\&+\text{-}0.0014$ **[ref. 11,12]**, $T_0 := 300\,K$. The Blackbody Radiation shift is assorted of uncertainty obtained with the squared of quadratic sum of $\delta(K_{BB})$, $\delta(\varepsilon)$ and $\delta(T)$:

$$\left(\frac{\delta(\nu)}{\nu_0}\right)_{Blackbody} = -1.6841\ 10^{-14} \pm 6.\ 10^{-17}$$

4 - Effect of the Microwave Spectrum effect and leakage effect

The clock frequency is measured as a function of the microwave power. Every 50 cycles the atom interrogation is alternated between 4 configurations of π/2, low density and high density, and 3π/2, low density and high density. It allows extrapolating and removing the variation of the collision shift in the comparison between π/2 and 3π/2 pulses. We find

$$\frac{(\delta(\nu))_{MicrowaveSpectrumLeakage}}{\nu_0} = 0.0 \pm 4.3\ 10^{-16}$$

5 - Measurement of the residual 1st order Doppler effect

We determined the frequency shifts caused by asymmetry of the coupling coefficients of the two microwave feedthroughs and the error on the launching direction by coupling the interrogation signal either “from the right” or “from the left” or symmetrically into the cavity. The measured shift is

$$\left(\frac{\delta(vu)}{\nu_0}\right)_{firstDoppler} = 4.5\ 10^{-15} \pm 3.0\ 10^{-16}$$

In FO2 fountain we feed the cavity symmetrically at 1% level both in phase and in amplitude. This shift is thus reduced by a factor of 100 and became negligible. The quadratic dependence of the phase becomes dominant. A worse case estimate based on **[ref. 6]** gives fractional frequency shift of 3 x 10^{-16} which we take as uncertainty due to the residual 1st order Doppler effect.

6 – Rabi and Ramsey effect and Majorana transitions effect

An imbalance between the residual populations and coherences of $m_F < 0$ and $m_F > 0$ states can lead to a shift of the clock frequency estimated to few 10^{-18} for a population imbalance of 10^{-3} that we observe in FO2 (see **[ref. 7]** and **[ref. 8]**).

7 – Microwave recoil effect

The shift due to the microwave photon recoil was investigated in **[ref. 3]**. It is smaller than 1,4 x 10^{-16} .

8 – Gravitational red-shift and 2nd order Doppler shift

The relativistic effect is evaluated as $\frac{(\delta(\nu))_{redshift}}{\nu_0} = \frac{g\,h}{c^2}$ with h=60m $\frac{(\delta(\nu))_{redshift}}{\nu_0} = 6.540\ 10^{-15} \pm \sigma_{Redshift} = 0.1\ 10^{-15}$

The 2nd order Doppler shift is less than 0,08 x 10^{-16} .

9 – Background collisions effect

The vacuum pressure inside the fountains is typically a few 10^{-8} Pa. Based on early measurements of pressure shift (see **[ref. 5]**) the frequency shift due to collisions with the background gas is < 10^{-16}.

See **[ref. 9]** for recent evaluations of systematic effects of FO2 fountain.

ANNEX 3

Uncertainty due to the dead time during the measurements

A statement of the distribution of the idle periods of measurements of FO2 is represented in figure 5,

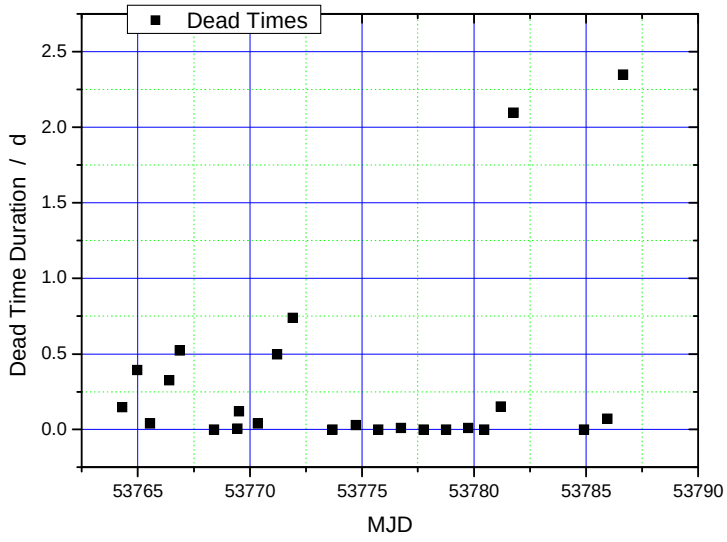

Figure 5: Dead Times on measurements of y(H_ Maser40 0890 –FO2) over the period MJD 53764 to 53789

For the period of the MJD 53764 until the MJD 53789 (29th January to 23th February), the variations of phase between hydrogen Maser 40 0890 and the hydrogen Maser 40 0889 were sampled every 1s. These phase variations are decimated by a factor of 100 to have a sampling time series of 100s. We have obtained the frequency variations after converting phase differences by frequency differences between H_Maser 40 0890 and the H_Maser 40 0889 plotted in figure 6. As we see a dead time in measurements is observed between MJD 53783,09 and MJD 53785,20 . We have taken the first time interval from MJD 53764 to 53783 without idle period. For calculating the Allan deviation in frequency and in time domain we have removed a frequency drift that we see in figure 6 and estimated to be -6,26 x 10^{-16} (see figure 7 and 8).

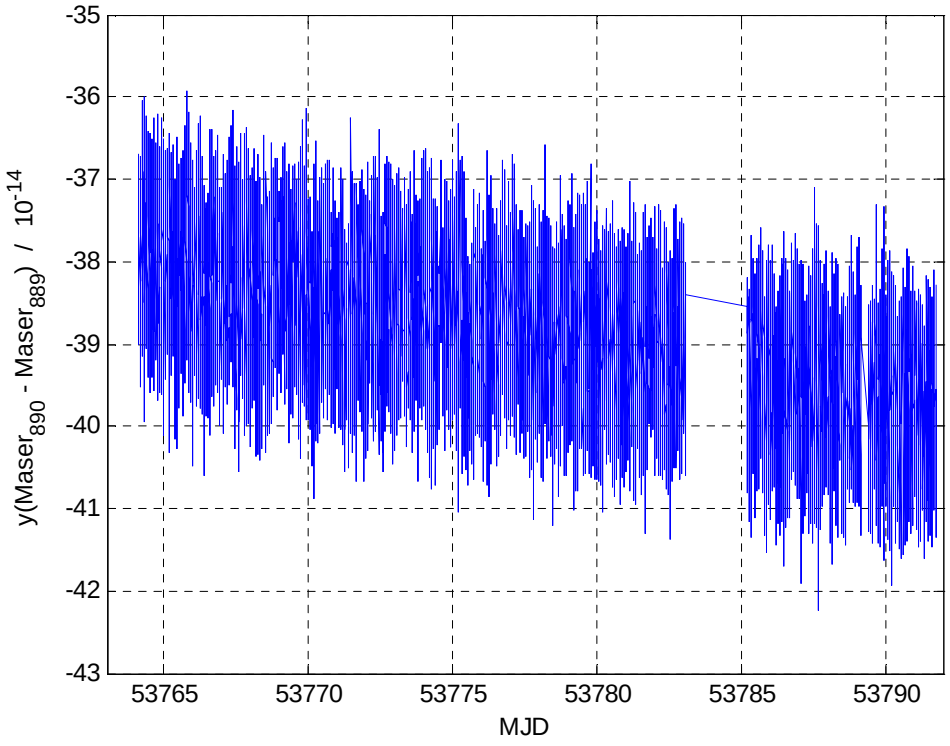

Figure 6: frequency differences y(Maser890-Maser889) MJD 53764 to 53789

Frequency stability analyses were performed using the overlapping Allan deviation on frequency data and represented from 29th January to 17th February 2006 in figure 7 and similarly time stability analyses with a time deviation were computed and represented in figure 8.

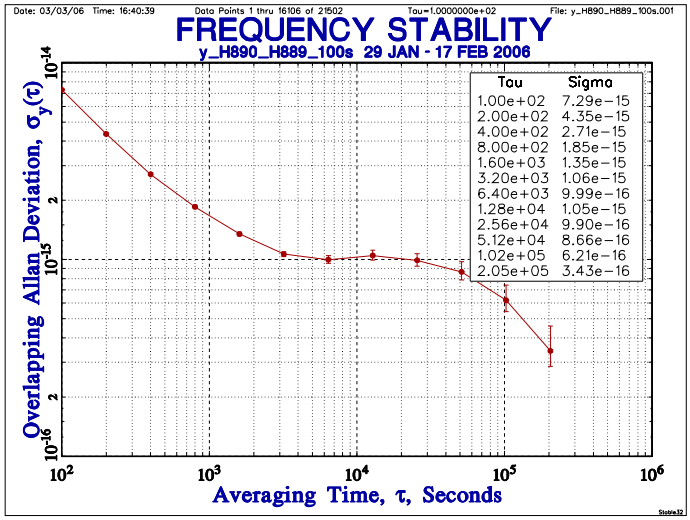

Figure 7: frequency stability analyzes x(HMaser890 - HMaser889) from MJD 53764 to 53789

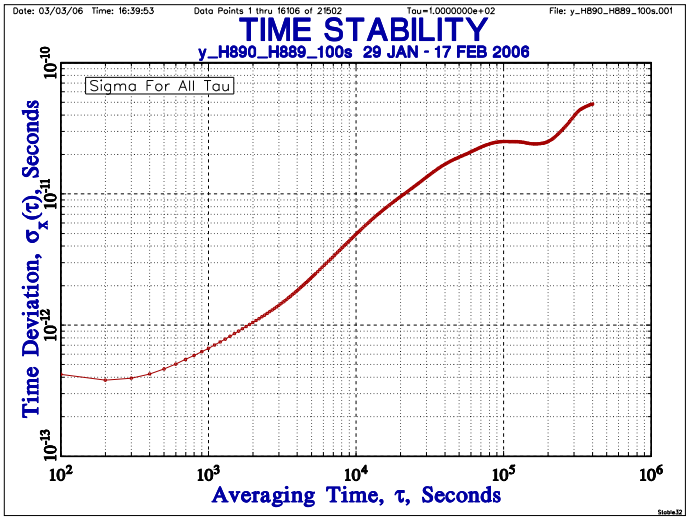

Figure 8: time stability analyzes from x(HMaser890 - HMaser889) from MJD 53764 to 53789

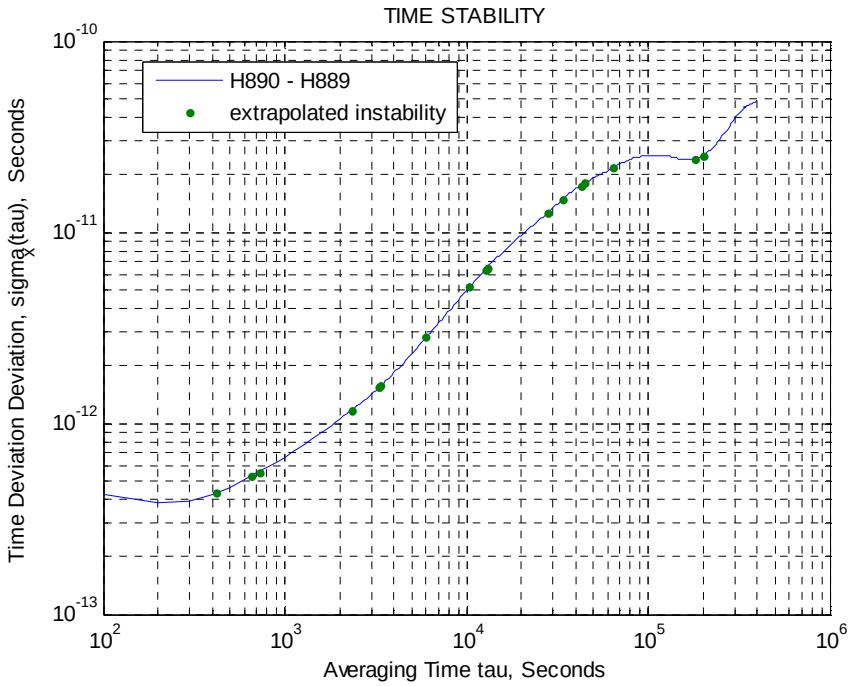

Figure 9: time stability analyzes from x(HMaser890 - HMaser889) from MJD 53764 to 53789 with extrapolated instability at dead time duration (See table 4)

Table 4 provides the standard deviations of the phase fluctuations of the hydrogen Maser 40 0890 with respect to the hydrogen Maser 40 0889 associated to each dead time according to their duration. Figure 9 shows the extrapolated instability of each dead time in our interval of measurements. The quadratic sum gives

$$\sum_{j=1}^{24} \sigma_x(\tau_m(j))^2 = 2.842\ 10^{-21}$$

The January February 2006 period of FO2 measurements is 22,9479 days or $T := 1982699$ seconds. We find the standard deviation of the fluctuations of frequency due to the dead times in measurements by the ratio

$$\sigma_{deadTime} = \frac{\sqrt{\sum_{i=1}^{24} \sigma_x(\tau_m(i))^2}}{T} = \quad \sigma_{deadTime} = 2.688\ 10^{-17}$$

End Date of each measurement (MJD)	Dead Time Duration second $\tau_m(i)$	$\sigma_x(\tau_m(i))$
53764.30903	12780	6.3741e-012
53764.97431	33900	1.49e-011
53765.55556	3300	1.5374e-012
53766.40764	28020	1.2656e-011
53766.88611	45120	1.8105e-011
53768.40556	0	0
53769.44236	420	4.3223e-013
53769.52153	10380	5.135e-012
53770.36111	3360	1.5621e-012
53771.22778	42780	1.7562e-011
53771.92292	63840	2.1649e-011
53773.69375	0	0
53774.72778	2340	1.1712e-012
53775.73403	0	0
53776.75	720	5.5495e-013
53777.75069	0	0
53778.74583	0	0
53779.75139	660	5.2987e-013
53780.45556	0	0
53781.20556	13020	6.4929e-012
53781.76042	1.8102e+005	2.4291e-011
53784.90139	0	0
53785.94653	6000	2.8133e-012
53786.65208	2.0286e+005	2.5319e-011

Table 4: Statement of the dead times of H_Maser 40 0890 - FO2 measurements between MJD 53764 to 53789

With taking $\sigma_{link\_Maser} = \sqrt{\sigma_{link\_lab}^2 + \sigma_{deadTime}^2}$ one obtains $\boxed{\sigma_{link\ Maser} = 1.035\ 10^{-16}}$

ANNEX 4

Linear Regression on the frequency measurements on period MJD 53764-53789

One calculates the linear regression by the algorithm of weighted least squares by statistical uncertainty of each frequency differences measurements:

$$y_k = a_1 + a_2\, t$$

Figure 10 gives the representation of frequency measurements and the linear fit resulting from weighted least squares by inverse of squares statistical uncertainty $1/\sigma_{Ai}^{\,2}$.

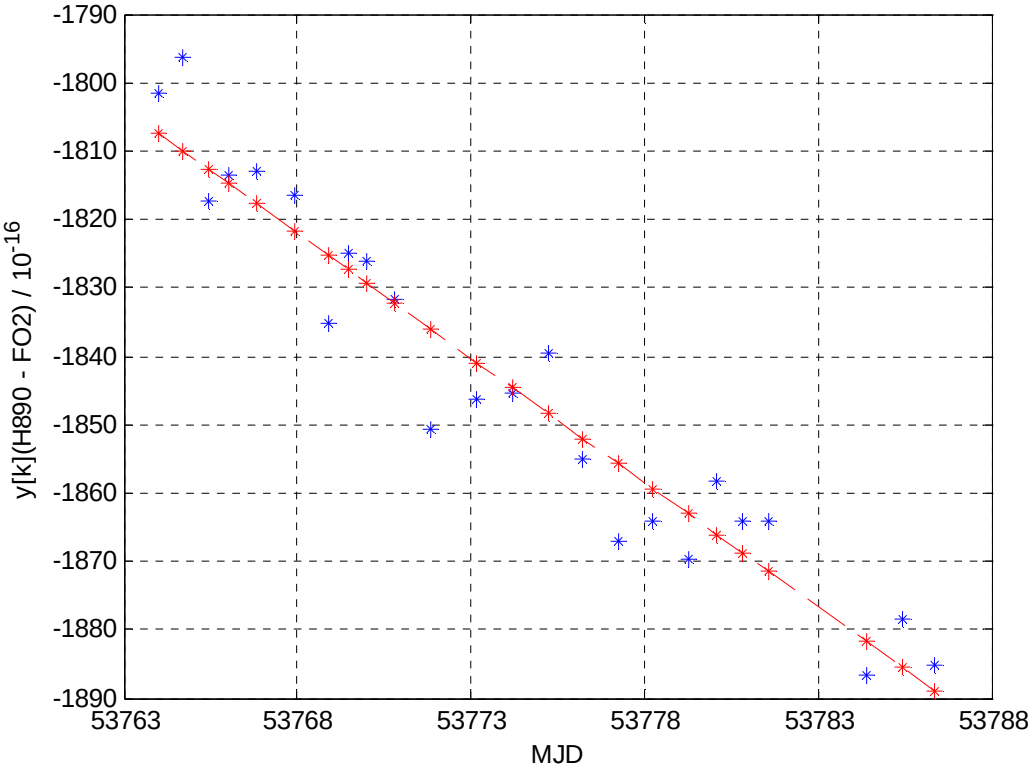

Figure 9: linear regression on the frequency y(HMaser-FO2) between MJD 53764 to 53789 weighted by uncertainty : $1/\sigma_{Ai}^{\,2}$

Summary of statistical terms:
Coefficient a1 = 1.94421123054228e-011
Coefficient a2 = -3.64981271667648e-016
sigma(a1) des yk de FO2 = 5.19133544619514e-013
sigma(a2) des yk de FO2 = 9.65376749816837e-018

Covariance Matrix :
2.69499637149221e-025 -5.01159450583263e-030
-5.01159450583263e-030 9.31952269086921e-035

mean date of measurements	=	**53776.5**	**from MJD start at 53764 & MJD ending at 53789**
Frequency mean by linear fit y_FO2	=	**-1.85303050412446e-013**	
Uncertainty propagation at t_moyen uc_y_FO2	=	6.0849297727384e-017	
Degree of Freedom DEF	=	22	
Mean Square Error = Chi2/DEF	=	5.55362722568962	
Birge ratio Rb (chi2/DEF)^1/2	=	2.35661350791546	
Limit of Birge ratio Rb = 1+sqrt(2/DEF)	=	1.30151134457776	
Probability of a sample y(Maser-FO2) being superior of Chi2|DEF	=	2.936938359131445e-016	
SSR Sum Square of Residues	=	1.16194763053803e-029	
RMS Root Mean Square of Residues	=	3.40873529412014e-015	
Allan Deviation at T with assumption of White Frequency Noise	=	**1.53634488667075e-016**	
T (seconds) = total duration	=	1982699.42400022	

$$\mathbf{y_{moy(H890\text{-}FO2)\_lin\_fit} = -1853{,}03 \times 10^{-16} \pm 1{,}53 \times 10^{-16}}$$

High order Polynomial fit on the frequency measurements on period MJD 53764-53789

One calculates the polynomial fit order M≥2 by the algorithm of least squares on each frequency differences measurements:

$$y = \sum_{i=0}^{M} p_{i+1}\, t^{(M-i)}$$

For 11 data measurements represented on figure 10, with interval duration of 1982699 seconds during MJD 53764,0-53789,0 period. With a polynomial of order M=5 we have smoothed the maser noise on 5 x *82612*s or about 5 days. We obtain the polynomial fit represented on figure 12.

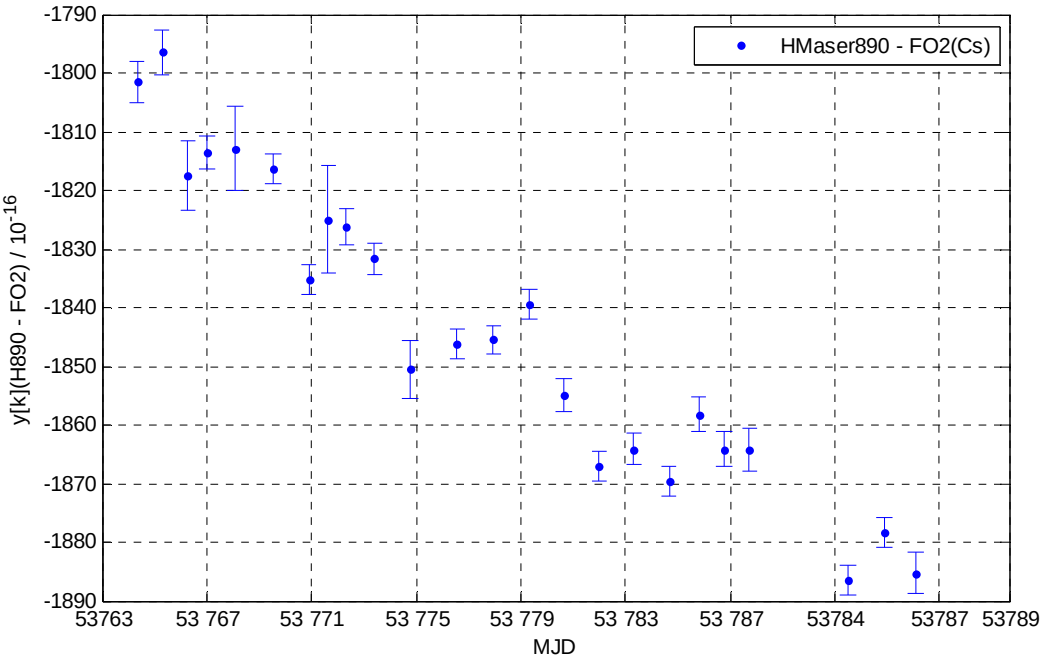

Figure 11: frequency differences & statistical uncertainties of y(H890-FO2), τ_0 = 82612s, MJD 53764 - 53789

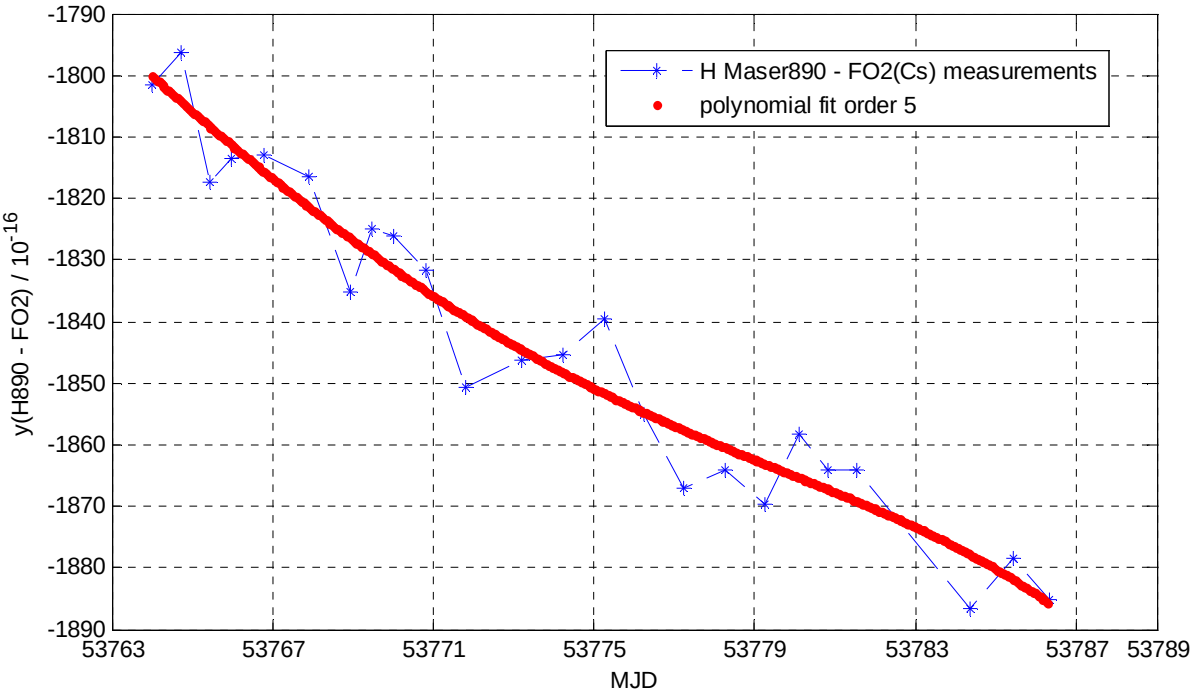

Figure 12: frequency differences y(H816-FO2) and the order 5 polynomial fit MJD 53764 - 53789

By integrating the fit polynomial from 53764 to 53789 we obtain an averaging frequency $\mathbf{y_{moy(H890\text{-}FO2)} = -1843{,}33 \times 10^{-16}}$.

Statistical uncertainty is evaluated by the frequency stability analysis of FO2 fountain. Figure 13 shows an overlapping Allan deviation for the residuals of linear fit and of polynomial fit and laws of white noise frequency modulation of 2,8 x $10^{-13}\tau^{-1/2}$ modelling of Maser noise and of 2,8 x $10^{-14}\tau^{-1/2}$ modelling of fountain noise limit An extrapolated value at the total duration 22.9479 days is obtained by law $\sigma_y(\tau\approx 23\ d)_{Maser} = 2{,}0 \times 10^{-16}$ representing the instability of Maser and law $\sigma_y(\tau\approx 23\ d)_{FO2} = 2{,}0 \times 10^{-17}$ representing FO2 noise with cryogenic oscillator.

By taking the fountain noise instability value extrapolated and added with the statistical uncertainty σ_A obtained from each measurement

$$\sigma_A = \sqrt{\frac{1}{\sum_{i=1}^{n} \frac{1}{\sigma_{Stat_i}^2 + \sigma_{Collision_i}^2}}}$$

resulting in $\sigma_A = 0{,}64 \times 10^{-16}$ we finally obtain the statistical uncertainty of mean frequency $\mathbf{y_{moy(H816\text{-}FO2)} = -1843{,}33 \times 10^{-16}}$ is:

$$u_A = \sqrt{\sigma_A^2 + \sigma_y(\tau = 23\ days)_{FO2}^2}$$

$$u_A = 6.401\ 10^{-17}$$

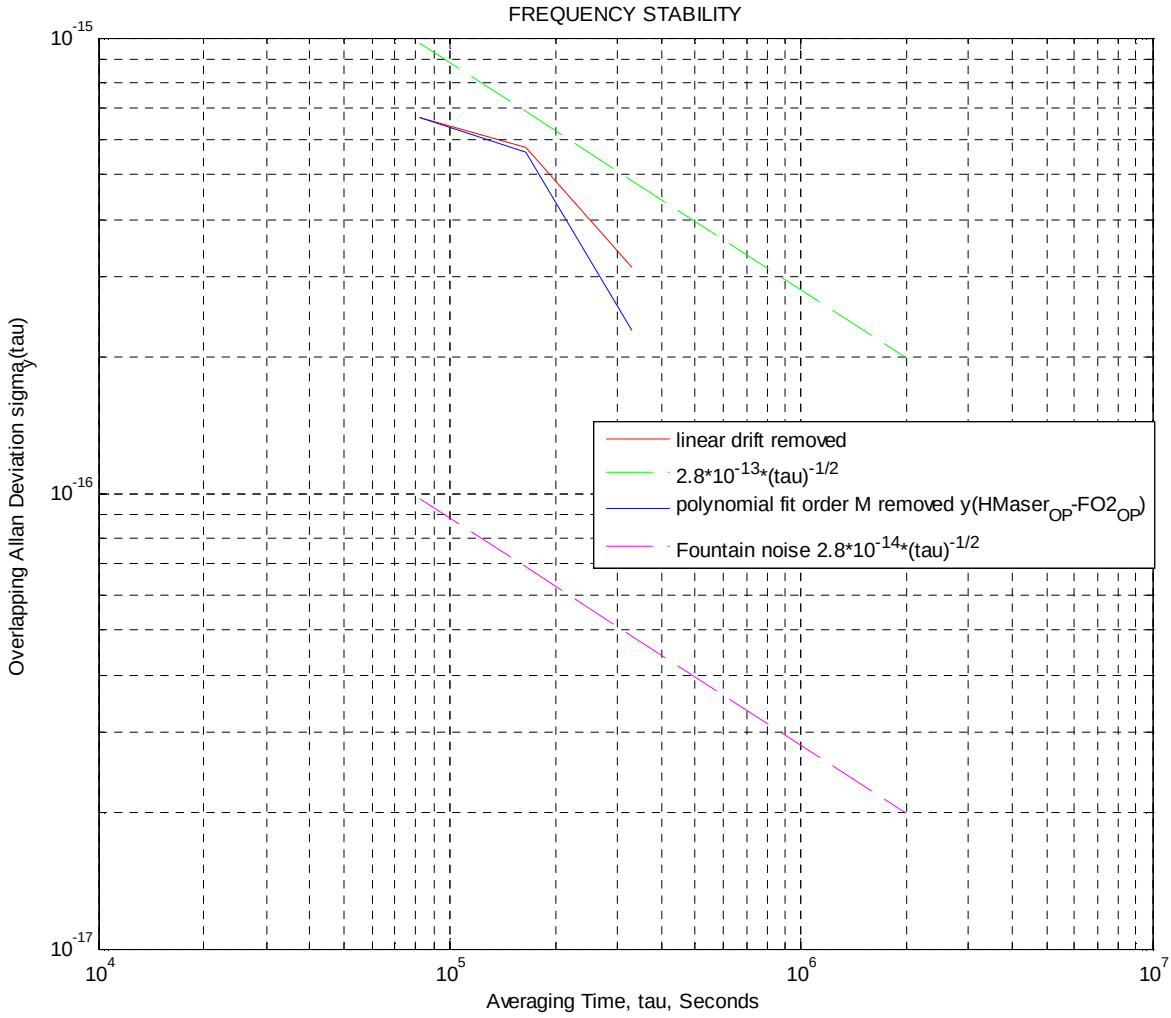

Figure 13: Comparison of frequency stability y(HMaser890 – FO2) polynomial order 1 and order M=5 removed from MJD 53764 to MJD 53789

ANNEX 5

Mean Frequency computed by phase differences

Figure 14 shows the evolution of the differences in fractional frequency y(t). At each period of integration is evaluated a frequency $\tilde{y}_k$ corresponding to the interval $t_{k+1} - t_k$. The relation binding the variations of phase and the instantaneous frequency deviations is given by

$$y_k = \frac{x_{k+1} - x_k}{t_{k+1} - t_k} \tag{1}$$

$$y(t) = \frac{\nu_{HMaser} - \nu_{FO2}}{\nu_0}$$

$\nu_0 = 9{,}192631770\ \text{GHz}$

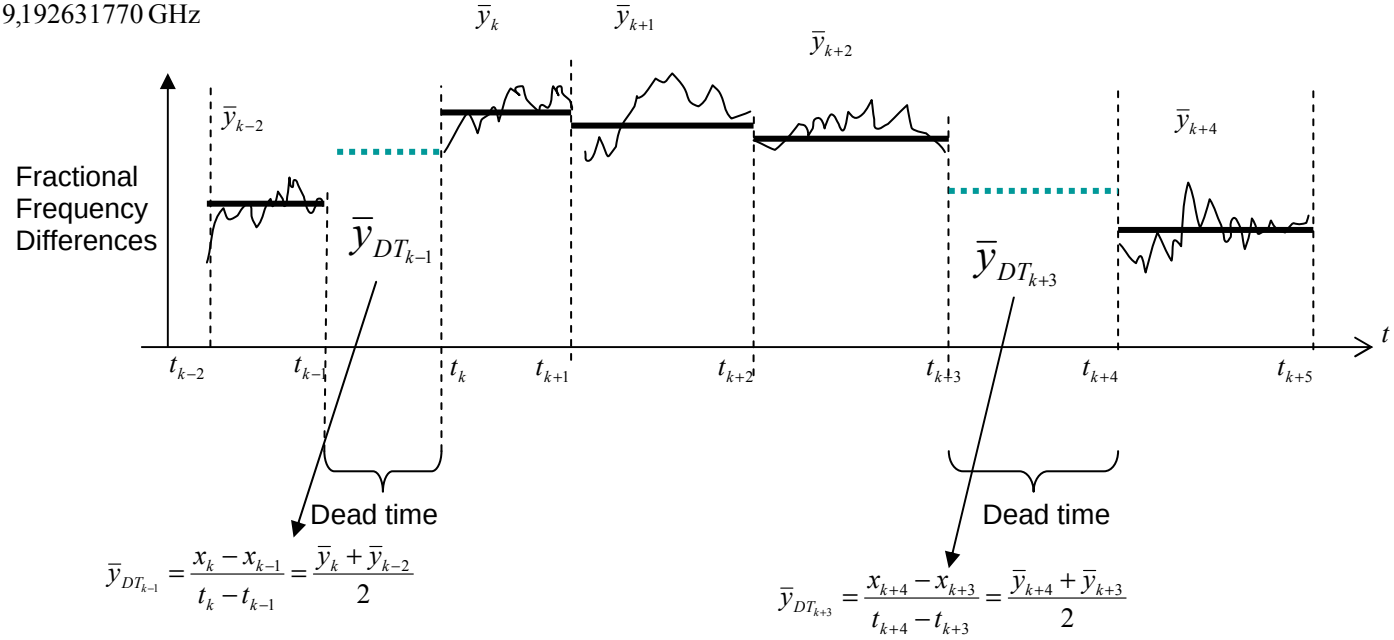

Figure 14: contribution of frequency measurements on the mean frequency calculated

By using equation (1) we have $x_{k+1} - x_k = (t_{k+1} - t_k)\, y_k$

and for addition of consecutive phase differences we find $\sum_{k=1}^{N} (x_{k+1} - x_k) = x_{N+1} - x_1 = \sum_{k=1}^{N} (t_{k+1} - t_k)\, y_k$

During the dead time we have evaluated the mean frequency by interpolating the mean frequency between two neighbouring intervals of integrations noted:

$$y_{DT_{m-1}} = \frac{1}{2} y_m + \frac{1}{2} y_{m-1} \tag{2}$$

The contributions of N duty intervals with the frequency measurements y_k and *M* idle intervals with the mean frequency extrapolating between two neighbouring intervals of integration y_{DT} give the summation

$$\left(\sum_{k=1}^{N} (t_{k+1} - t_k)\, y_k \right) + \left(\sum_{m=1}^{M} (t_{m+1} - t_m)\, y_{DT_m} \right) = x_{fin} - x_{deb} \tag{3}$$

$$\boxed{y_{moy} = \frac{x_{fin} - x_{deb}}{86400\ MJD_{fin} - 86400\ MJD_{deb}}} \tag{4}$$

Where $(x_{fin} - x_{deb})$ represents the phase variation between the whole period of integration.

The evaluation of statistical uncertainty on each phase differences data extracted from fractional frequency differences, as we have in presence of white frequency noise (WFM) in each period of measurement, is given by the expression

$$\sigma_x(\tau_i)^2 = \sigma_y(\tau_i)^2 \tau_i^2$$

For the whole period T of measurement that gives in frequency instability

$$\sigma_y(\tau) = \frac{\sqrt{\sum_{i=1}^{N} \sigma_y(\tau_i)^2 \tau_i^2}}{T}$$

With N =25, from the 29th January to 23rd February 2006 and $T = 86400\ MJD_{fin} - 86400\ MJD_{deb}$ =

$T := 1982699$ seconds it gives

$$\sigma_y(\tau) = \frac{\sqrt{\sum_{i=1}^{25} \sigma_y(\tau_i)^2 \tau_i^2}}{T} = 0.466\ 10^{-16}$$

$$\boxed{\sigma_y = 4.733\ 10^{-17}}$$

The evaluation of the mean frequency between two intervals of integrations during the period from MJD 53764 to MJD 53789 is given by equation (2) and calculated for frequency fluctuation difference measurements. Figure 15 shows the frequency differences between H_Maser 40 0890 and FO2 (blue plus) and the mean frequency during dead times (magenta stars).

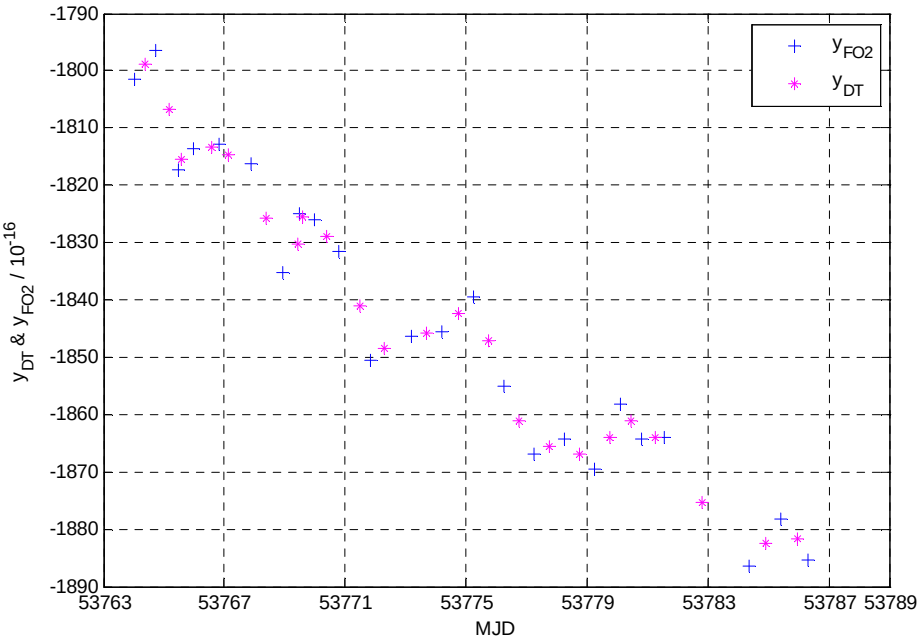

Figure 15: frequency differences H_Maser40 0890 and FO2 from MJD 53764 up to MJD 53789

From equation (3) we find the phase difference over the whole period of integration

$$x_{fin} - x_{deb} = -.366448\ \mu s$$

This value is replaced in equation (4) above for computation of y_{moy} during this period. We find

$$\boxed{y(Maser_{890} - FO2) = -1.84823\ 10^{-13}}$$

REFERENCES

[ref. 1] - C. Vian, P. Rosenbusch, H. Marion, S. Bize, L. Cacciapuoti, S. Zhang, M. Abgrall, D. Chambon, I. Maksimovic, P. Laurent, G. Santarelli, A. Clairon of Obs. Paris, SYRTE, A. Luiten, M. Tobar, Univ. W. of Australia School of Physics, C. Salomon of LKB, "LNE-SYRTE Fountains: Recent Results", **CPEM 2004, Proceedings IEEE Transactions on Instrumentation & Measurement, Vol. 54, N0. 2, April 2005.**

[ref. 2] - F. Pereira Do Santos, H. Marion, M. Abgrall, S. Zhang, Y. Sortais, S. Bize, I. Maksimovic, D. Calonico, J. Grünert, C. Mandache, C. Vian, P. Rosenbusch, P. Lemonde, G. Santarelli, Ph. Laurent and A. Clairon of LNE-SYRTE, C. Salomon of LKB, "Rb and Cs Laser Cooled Clocks: Testing the Stability of Fundamental Constants". **Proceedings IEEE 2003, EFTF Tampa May 2003, p 55-67.**

[ref. 3] - P. Wolf of LNE SYRTE, C.J. Bordé of LPL, "Recoil effects in microwave Ramsey spectroscopy", arxiv: **quant-ph/0403194**.

[ref. 4] - F. Pereira Do Santos, H. Marion, S. Bize, Y. Sortais, A. Clairon, and C. Solomon "Controlling the Cold Collision Shift in High Precision Atomic Interferometry" of, **Phys, Rev, Lett, 89,233004 (2002)**.

[ref. 5] - J. Vanier, C. Audouin, « The Quantum Physics of Atomic Frequency Standards », **Adam Hilger, Bristol & Philadelphia (1989)**.

[ref. 6] - R. Schröder, U. Hübner and D. Griebsch, "Design and Realization of the Microwava Cavity in PTB Caesium Atomic Clock CSF1" **IEEE Trans. Instrum. Meas., vol. 49, p.383, 2002**.

[ref. 7] - L. Cutler *et al*, "Frequency pulling by hyperfine σ - transitions in cesium atomic frequency standards, **J. Appl. Phys. Vol. 69, pp. 2780, 1991**.

[ref. 8] - A. Bauch, R. Schröder "Frequency shift in Caesium Atomic Clock due to Majorana transitions", Annalen der Physik**, vol. 2, pp. 421, 1993**.

[ref. 9] – H. Marion thèse de doctorat de l'Université de Paris 6 (Mars 2005)